Title
SINTERING OF PARTICULATE COMPOSITES UNDER A UNIAXIAL STRESS

Authors
Rahaman, M.N.
DeJonghe, L.C.

Publication Date
1989-05-01

LBL-26921
Preprint

Center for Advanced Materials

CAM

Submitted to Journal of the American Ceramics Society

Sintering of Particulate Composites Under a Uniaxial Stress

M.N. Rahaman and L.C. De Jonghe

May 1989

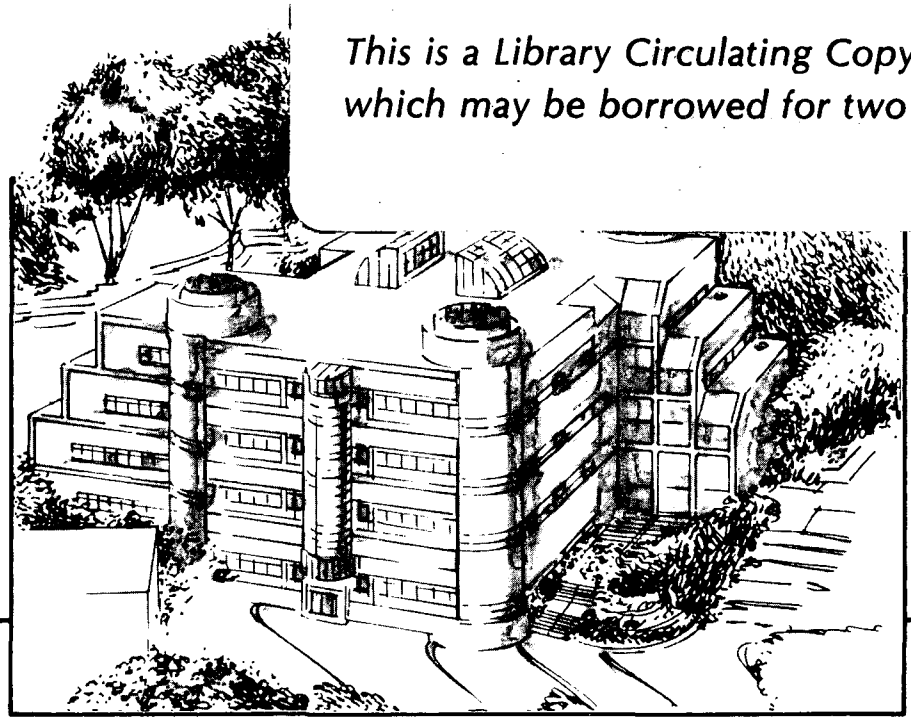

Materials and Chemical Sciences Division

Lawrence Berkeley Laboratory • University of California

ONE CYCLOTRON ROAD, BERKELEY, CA 94720 • (415) 486-4755

Prepared for the U.S. Department of Energy under Contract DE-AC03-76SF00098

DISCLAIMER

LBL # 26821

SINTERING OF PARTICULATE COMPOSITES UNDER A UNIAXIAL STRESS

Mohamed N. Rahaman*,# and Lutgard C. De Jonghe*,$

Materials and Chemical Sciences Division, Lawrence Berkeley Laboratory, One Cyclotron Road, University of California, Berkeley, California 94720

Supported by the Division of Materials Sciences, Office of Basic Energy Sciences, U.S. Department of Energy, under Contract No. DE-AC03-76SF00098.

*Member, the American Ceramic Society.

#Permanent address: The University of Missouri-Rolla, Ceramic Engineering Department, Rolla, Missouri 65401

$Also with the Department of Materials Science and Mineral Engineering, University of California, Berkeley, California 94720

Abstract

The sintering of particulate composites consisting of a fine-grained zinc oxide matrix and < 10 volume percent of coarse silicon carbide inclusions was investigated at 725°C under a uniaxial stress of ≈ 250 kilopascal. Data for the densification and creep rates of the composite were compared with those for the unreinforced matrix. The inclusions cause a drastic reduction in the measured density and creep rates. They have a greater effect on the densification process, however; the ratio of the densification rate to the creep rate of the composite is approximately half that of the unreinforced compact. The factors that cause the reduction in this ratio are present from the very early stage of sintering. The consequences of the present data for the processing of polycrystalline ceramic matrix composites are discussed.

I. Introduction

Conventional, pressureless sintering is potentially a more economical process for fabricating ceramic matric composites, compared to hot pressing or hot isostatic pressing techniques. Considerable difficulties are often encountered, however, in sintering composites to the high matrix density normally required for many technological applications. Thus, numerous efforts, both theoretical and experimental, have been made within the past five years to understand these difficulties at a fundamental level so that the conventional sintering process can be better applied to the fabrication of composite materials. Most theoretical work employed a model system consisting of a fine-grained matrix containing coarse, inert, rigid inclusions since this is the system of interest for ceramic matrix composites.

Rahaman and De Jonghe[1,2] studied the sintering of particulate composites containing a polycrystalline matrix (ZnO) or an amorphous matrix (soda-lime glass) and inclusions of SiC. For the amorphous matrix composite, the densification rate obeyed the rule of mixtures when the inclusion volume fraction, v_i, was less than 0.1, and could be described very well by Scherer's theory[3] of sintering with rigid inclusions for $v_i > 0.15$. Above this value rigid network formation, which was not taken into account in Scherer's theory, appeared to be the main cause of the deviation from theory.

In contrast, the SiC inclusions drastically reduced the densification rate of the polycrystalline ZnO matrix composite even at quite low inclusion content (>5 v%). Similar data have been obtained recently by Bordia and Raj[4] for TiO_2-Al_2O_3 composites and by Brook et al[5] for Al_2O_3-Al_2O_3 composites. The data for the polycrystalline matrix composite can at first sight be explained[6] in terms of the large viscoelastic backstresses predicted by the theories of Raj and Bordia[7] and Hsueh et al.[8] However, Scherer's

theory[3] and an analysis by De Jonghe and Rahaman[9] have cast serious doubts on this explanation since they showed that the backstresses were small. Thus, other explanations need to be looked at.

A number of suggestions have been put forward recently to account for the drastic reduction in the densification rates of polycrystalline matrix composites. A geometric model proposed by Lange[10] involved constrained sintering of the matrix due to network formation of the inclusions. This model cannot readily account for the differences in densification behavior between glass and polycrystalline matrices. In addition, it is improbable that the inclusions would form a continuous network for $v_i < 0.1$; the data of Rahaman and De Jonghe[2] for glass matrix composites show quite clearly that network formation is unimportant below this value of v_i.

Another explanation put forward by Lange[11] attributed the drastic reduction in the densification rates of polycrystalline matrix composites to "damage" (e.g. voids) in the matrix produced by non-uniform densification. Damage should be most severe in the matrix regions nearest the inclusions where the hoop stresses are largest, but can also result from non-uniform packing of the matrix or from the cold compaction process. Since these voids may not close, they may limit severely the densification rate and the end point density. There is, at present, no direct experimental evidence to support this explanation.

Finally, Bordia and Scherer[12] have identified a number of other factors that can lead to the drastic retardation of the densification rates in polycrystalline matrix composites. These included the competition between densification and coarsening, and the development of anisotropies in the densification rate and the shear and bulk moduli. The anisotropies result from the different stress fields in the radial and hoop directions experienced by the shrinking matrix. Competition between densification and coarsening, however, is unlikely to be a valid mechanism since it is also present in

the unreinforced matrix; in addition, when the densification rates in the matrix are compensated for grain growth, there is still a large deviation from theory.[13]

The present work entails a study of the effect of rigid inclusions on the simultaneous creep and densification of a model polycrystalline powder matrix (zinc oxide). A low uniaxial stress is applied to a composite containing > 10 v% inclusions to produce measurable creep but almost no change in the densification during sintering. It is important to understand how the inclusions influence both processes since the transient stresses developed during sintering can be relaxed by creep.

II. Experimental Procedure

A fine-grained ZnO powder[#], average grain size ≈ 0.4 μm, and SiC powder*, classified to a narrow size range about an average of ≈ 12 μm, were used as the matrix and inclusions, respectively. The amount of SiC was chosen to give an inclusion volume fraction of 0.1 based on the fully dense composite. The powders were mixed in chloroform and stir-dried, then disrupted using a mortar and pestle, and finally die-pressed to give composite green compacts (6 mm in diameter by 6 mm) with the same matrix density of ≈ 0.44 of the theoretical. For comparison, unreinforced compacts with the same density were formed by a similar method.

The samples were sintered in air for 2 h in a loading dilatometer[14]; the instrument allowed the continuous monitoring of the axial shrinkage and the application of a constant uniaxial load. Sintering was performed at 725^{0}C and under uniaxial stresses of 0 and ≈ 250 kPa. The mass and dimensions of the

---

[#]Reagent Grade, Mallinckrodt Inc., Paris, KY.
*Union Carbide Corp., New York, NY.

samples were measured before and after sintering. In a separate set of experiments sintering was terminated after times between 0 and 2 h and the dimensions of these compacts were measured using a micrometer.

III. Data Analysis

The experiments give data for the axial and radial shrinkage from which the true strains in the axial and radial directions, ϵ_z, and ϵ_r, respectively, were calculated according to the equations

$$\dot{\epsilon}_z = d[\ln(L/L_o)]/dt \qquad (1)$$

$$\dot{\epsilon}_r = d[\ln(R/R_o)]/dt \qquad (2)$$

where L_o and R are the initial length and radius, respectively, and L and R are the corresponding time-dependent values.

The creep strain rate, $\dot{\epsilon}_c$, and the volumetric strain rate, $\dot{\epsilon}_\rho$, were evaluated according to the relations

$$\dot{\epsilon}_c = (2/3)(\dot{\epsilon}_z - \dot{\epsilon}_r) \qquad (3)$$

$$\dot{\epsilon}_\rho = \dot{\rho}/\rho = -(\dot{\epsilon}_z + 2\dot{\epsilon}_r) \qquad (4)$$

where ρ is the relative density.

If D_o and D are the initial and time-dependent overall density, respectively, of the reinforced sample, then the density of the matrix phase at any time is[2]

$$D_m = D(D_o - v_{io}D_i)/(D_o - v_{io}D) \qquad (5)$$

where D_i is the invariant density of the inclusion phase and v_{io} is the initial inclusion volume fraction. The volumetric strain rate of the matrix is

$$\dot{\epsilon}_{\rho m} = (D/D)(1 - v_{io}D/D_o) \qquad (6)$$

The current volume fraction of the inclusion phase, v_i, is based on the total volume of the compact, which includes the void phase; as the void phase disappears during sintering, v_i increases. Usually the volume

fraction of the inclusion phase is calculated on the basis of the fully dense composite, denoted here by v_{if}. Then v_i is related to v_{if} according to the relation

$$v_i = \rho_m[\rho_m + (1 - v_{if})/v_{if}]^{-1} \qquad (7)$$

The axial stress on the sample, σ_z, was measured from the constant applied load, P, and the change in cross-sectional area of the sample according to the relation

$$\sigma_z = (P/A_o)\exp(-2\epsilon_r) \qquad (8)$$

where A_o is the initial area of the sample. For these experiments the spring load required to keep the dilatometer pushrod in contact with the sample was < 3% of the applied load and was neglected.

IV. Results

Figure 1 shows the axial strain, ϵ_z, vs time, t, for the unreinforced sample and the sample reinforced with 10 volume percent (v%) inclusions (i.e. based on the fully dense composite). The samples were sintered in air for 2 h at 725°C and under uniaxial stresses of 0 and 250 kPa (based on the initial sample). The time t = 0 represents the beginning of shrinkage and the "isothermal" sintering temperature was reached after t = 6 min; each curve is the average of two runs under identical conditions and each is reproducible to within ± 2%. The significant reduction in ϵ_z for the reinforced sample is comparable to earlier observations[1,15] on the same system.

Data for ϵ_z vs the radial strain, ϵ_r, are shown in Fig. 2 for the unreinforced and reinforced samples that were sintered under uniaxial stresses of 0 and 250 kPa. The shrinkage of the samples sintered under zero stress is almost isotropic. Under the same applied stress, the shrinkage anisotropy of the reinforced sample is greater than that of the unreinforced sample.

The relative density of the unreinforced and reinforced samples, ρ_u and ρ_{re}, respectively, are shown in Fig. 3 as a function of time. The theoretical densities of ZnO and a composite of ZnO containing 10 v% SiC inclusions are 5.60 and 5.36 g/cm^3, respectively. The drastic reduction in the density of the reinforced sample compared to the unreinforced one after the same sintering time is very evident. The applied uniaxial stress is much lower than the sintering stress (due to reduction in surface area) and does not produce any measurable increase in the density.[16] Figure 4 shows the creep strain for the unreinforced and reinforced samples, ϵ_{cu} and ϵ_{cre}, respectively, as a function of time; for the uniaxial stress used ($\approx$ 250 kPa for both samples), ϵ_{cu} and ϵ_{cre} are approximately the same.

As pointed out earlier, the current inclusion volume fraction, v_i, increases during sintering as the void phase disappears. Equation (7) was used to calculate v_i as a function of the relative density of the matrix, ρ_m, and the data are shown in Figure 5. During sintering, ρ_m increases from 0.44 to 0.63 which leads to an increase in v_i from 0.046 to 0.066.

The densification and creep rates of the unreinforced sample ($\dot{\epsilon}_{\rho u}$ and $\dot{\epsilon}_{cu}$, respectively) and of the reinforced sample ($\dot{\epsilon}_{\rho re}$ and $\dot{\epsilon}_{cre}$, respectively) were calculated by fitting smooth curves to the data of Figs. 3 and 4 and differentiating. The results are shown in Fig. 6 as a function of ρ_m. At a given density both the densification rate and the creep rate of the reinforced sample are drastically lower than those for the unreinforced material. The extent of the reduction increases with increasing density. Grain growth contributes to this reduction but even if the rates were compensated for grain growth, the densification rates of the reinforced sample would still be drastically lower than what can be reasonably expected on the basis of a theoretical calculation of the viscous backstresses.[9]

The ratio of the densification rate to the creep rate can also be

measured. The creep rates $\dot{\epsilon}_{cu}$ and $\dot{\epsilon}_{cre}$ were compensated for the change in cross-sectional area of the sample [Eq. (8)], and then normalized to a constant stress of σ_z = 200 kPa by assuming that the creep rate was proportional to σ_z. The data for the unreinforced and the reinforced samples, $\dot{\epsilon}_{\rho u}/(3\dot{\epsilon}_{cu})$ and $\dot{\epsilon}_{\rho re}/(3\dot{\epsilon}_{cre})$, respectively, are shown in Fig. 7 as a function of ρ_m. The data are relatively independent of density and this is consistent with earlier work on a number of polycrystalline and glass systems.[9] An interesting feature is that the ratio of the densification to the creep rate for the reinforced sample is approximately 2 times lower than that for the unreinforced sample.

V. Discussion

It is evident from Fig. 7 that the ratio of the densification rate to the creep rate is relatively constant even from the beginning of "isothermal" sintering. A small amount of densification occurs during the heat-up stage (ρ_m increases from the initial value of 0.44 to 0.48) and the corresponding data have been excluded. However, it appears unlikely that the ratio of the densification rate to the creep rate would change significantly during heat-up. Indeed, in constant heating rate sintering which allows a more accurate measurement in the earliest stages of sintering, this ratio has also been found to be constant.[17] It must therefore be concluded that the factors leading to the reduction in the ratio of the densification rate to the creep rate for the reinforced sample are present from the very onset of sintering.

A striking aspect of the data is that the time dependence of the creep rate is hardly affected by the presence of the inclusions, while the densification rate is noticeably decreased (Figs. 3 and 4). In the context of expressions for densification and for creep of particulate composite systems, this observation restricts the number of possible

causes that may lead to the strong lowering of the densification rate by a relatively low volume fraction of inclusions. For a powder compact creeping under a low uniaxially applied stress, the creep rate may be expressed as [9,16]

$$\dot{\epsilon}_c = KD(kTX^n)^{-1}\sigma_a\phi^{(n+1)/2} = \sigma_a/\eta_c \qquad (9)$$

where K is a constant, D is a diffusion coefficient, k is the Boltzmann constant, T is the absolute temperature, X is the average pore spacing, n is a constant that depends on the mechanism of mass transport (e.g. n = 3 for grain boundary diffusion and n = 2 for volume diffusion), σ_a is the applied uniaxial stress, ϕ is a stress intensification factor[18,19], and η_c is the creep viscosity. Similarly, defining the sintering stress, Σ, as an equivalent externally applied stress, then the densification rate may be expressed as

$$\dot{\epsilon}_\rho = \Sigma/\eta_\rho \qquad (10)$$

where η_ρ is the densification (or bulk) viscosity.*

The sintering stress may be modified by a number of factors, including the hydrostatic backstresses from rigid inclusions. Model considerations as well as experiments[3,9] suggest strongly that the creep viscosity and the densification viscosity are intimately related. Although the creep viscosity and the densification viscosity have as yet not been measured independently for ceramic powder compacts, it is plausible that the indifference of the initial creep viscosity to the presence of the dispersed phase should be similarly reflected in the initial densification viscosity. It can therefore be argued that the relative decrease in the initial densification rate resides in the decrease of the sintering stress, Σ, rather

*(In a number of earlier publications, e.g. references 1,2,9 and 16, the sintering stress was written as Σ/ϕ while in others, e.g. reference 8, the same stress was written as Σ. The current symbolism for the equivalent externally applied stress is now adopted; the mean grain boundary stress will now be $\Sigma\phi$ rather than Σ.)

than in an increase in the densification viscosity. Such a decrease must then be due to an effect that can be expressed as a quasi-hydrostatic backstress, σ_{back}, opposing Σ. However, the backstress resulting from the mismatch in the densification strain rate between the matrix and the rigid inclusions, σ_{incl}, cannot be proposed as being the main component of σ_{back} since reasonable model considerations[3,9] indicate clearly that σ_{incl} is only a viscous backstress, equal to $\approx v_i\Sigma$, where v_i is the inclusion volume fraction. At the same time, it is doubtful that at the low v_i considered here a constrained network model[10] can be invoked, as pointed out earlier.

The observation of the decreased densification rate from the earliest stages of densification indicates that its causes are also present from the beginning, and have to be sought in differences in matrix microstructure brought about during the compaction process or in the spacial distribution of the dispersed phase, along the lines proposed by Lange[11]. While much work still remains to identify unambiguously the causes of the drastic reduction in the densification rate, it could be appreciated that the random distribution of the dispersed phase will, in turn, introduce spacial variations in the green density of the matrix. Indeed, in die compaction, a matrix region with a statistically higher concentration of dispersoids will have to be compacted more than the average green density, and conversely. Increased spacial variations of the matrix density will result in increased differential densification which generally leads to a decrease in the overall densification rate. Another possibility, also leading to increased differential densification, arises if similar green density variations would lead to microcrack formation in the green compact upon unloading in die compaction. This microcracking results from the differences in the elastic compressibility of regions in the compact with different average density and hence different elastic moduli, and clearly will be significantly less or absent in slip casting,

if damage from drying shrinkage can be suppressed. It should also decrease with increasing green compact strength. Both modelling and experiments need to be carried further to consider the consequences of these possibilities. All the proposed explanations, however, clearly point in a direction that would predict significantly less effects of the dispersed phase on the densification of particulate ceramic matrix composites with uniform, ordered distributions of the dispersed phase compared to those distributions resulting from random mixing, or even more commonly, imperfect mixing with clustering.

VI. Conclusions

The present work in which a polycrystalline ZnO matrix containing < 10 volume percent SiC inclusions was sintered under a low uniaxial stress shows that the inclusions cause a reduction by a factor of ≈ 2 in the ratio of the densification rate to the creep rate.

When grain growth is taken into account, the inclusions cause a reduction in the densification rate (i.e. by a factor of ≈ 2) without seriously affecting the creep rate.

The mechanism that leads to the reduction in the densification rate starts operating in the very early stage of sintering.

Acknowledgement: Discussions with R. J. Brook have been greatly appreciated.

References:

1. L. C. De Jonghe, M. N. Rahaman, and C. H. Hsueh, "Transient Stresses in Bimodal Compacts During Sintering," Acta Metall., 34 [7] 1467-71 (1986).

2. M. N. Rahaman and L. C. De Jonghe, "Effect of Rigid Inclusions on the Sintering of Glass Powder Compacts," J. Am. Ceram. Soc., 70 [12] C-348 - C-351 (1987).

3. G. W. Scherer, "Sintering with Rigid Inclusions," J. Am. Ceram. Soc., 70 [10] 719-25 (1987).

4. R. K. Bordia and R. Raj, "Sintering of TiO_2- Al_2O_3 Composites: A Model Experimental Investigation," J. Am. Ceram. Soc., 71 [4] 302-10 (1988).

5. R. J. Brook, W. H. Tuan, and L. A. Xue, "Critical Issues and Future Directions in Sintering Science," pp. 811-23 in Ceramic Transactions: Ceramic Powder Science II. Edited by G. L. Messing, E. R. Fuller, and H. Hausner. The American Ceramic Society, Westerville, OH (1988).

6. R. K. Bordia and R. Raj, "Analysis of Sintering of a Composite with a Glass or Ceramic Matrix," J. Am. Ceram. Soc., 69 [3] C-55 - C-57 (1986).

7. R. Raj and R. K. Bordia, "Sintering Behavior of Bimodal Powder Compacts," Acta Metall., 32 [7] 1003-19 (1984).

8. C. H. Hsueh, A. G. Evans, R. M. Cannon and R. J. Brook, "Viscoelastic Stresses and Sintering Damage in Heterogeneous Powder Compacts," Acta Metall., 34 [5] 927-36 (1986).

9. L. C. De Jonghe and M. N. Rahaman, "Sintering Stress of Homogeneous and Heterogeneous Powder Compacts," Acta Metall., 36 [1] 223-29 (1988).

10. F. F. Lange, "Constrained Network Model for Predicting Densification Behavior of Composite Powders," J. Mater. Res., 2 [1] 59-65 (1987).

11. F. F. Lange, "Densification of Powder Rings Constrained by Cylindrical Cores," Paper presented at the 90th Annual Meeting of the American Ceramic Society, Cincinnati, OH, May 1-5, 1988.

12. R. K. Bordia and G. W. Scherer, "Constrained Sintering: III, Rigid Inclusions," Acta Metall., in press.

13. M. N. Rahaman and L. C. De Jonghe, "Effect of Rigid Inclusions on Sintering," pp. 887-96 in Ceramic Transactions: Powder Science II. Edited by G.L. Messing, E. R. Fuller, and H. Hausner. The American Ceramic Society, Westerville, OH (1988).

14. L. C. De Jonghe and M. N. Rahaman, "A Loading Dilatometer," Rev. Sci.

Instrum., 55 [12] 2007-2010 (1984).

15. M. W. Weiser and L. C. De Jonghe, "Inclusion Size and Sintering of Composite Powders," J. Am. Ceram. Soc., 71 [3] C-125 - C-127 (1988).

16. M. N. Rahaman and L. C. De Jonghe, "Creep-Sintering of Zinc Oxide," J. Mater. Sci., 22 4326-30 (1987).

17. M.-Y. Chu, L. C. De Jonghe, and M. N. Rahaman, "Effect of Temperature on the Densification/Creep Rate During Sintering," Acta Metall., in press.

18. W. Beere, "A Unifying Theory of the Stability of Penetrating Liquid Phases and Sintering Pores," Acta Metall., 23 [1] 131-38 (1975).

19. J. M. Vieira and R. J. Brook, "Kinetics of Hot-Pressing: The Semilogarithmic Law," J. Am. Ceram. Soc., 67 [4]245-49 (1984).

Figure Captions

Fig. 1. Axial strain vs time for unreinforced ZnO (referred to as sample U) and ZnO reinforced with 10 v% SiC (sample R) sintering at 725°C under uniaxial stresses of 0 and 250 kPa.

Fig. 2. Axial strain vs radial strain for the experiments described in Fig. 1.

Fig. 3. Relative density vs time for samples U and R.

Fig. 4. Creep strain vs time for samples U and R.

Fig. 5. Inclusion volume fraction vs the relative density of the matrix for sample R.

Fig. 6. Volumetric densification rate, $\dot{\rho}/\rho$, and creep strain rate, $\dot{\epsilon}_c$, vs relative density of the matrix for the experiments described in Fig. 1.

Fig. 7. Ratio of the volumetric densification rate to the creep rate (normalized at a constant stress of 200 kPa) vs relative density of the matrix for samples U and R.

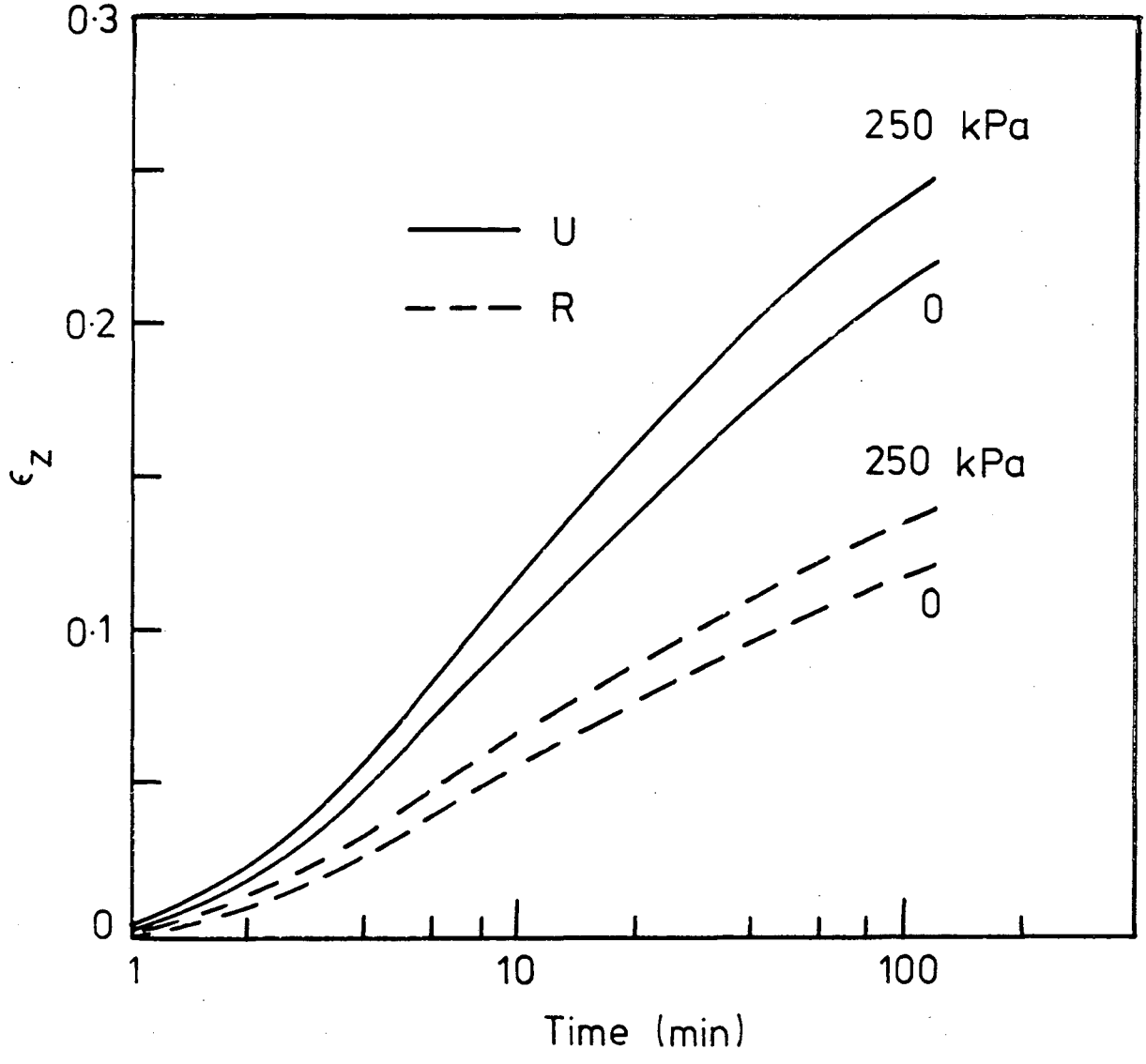

XBL 893-906

Fig. 1

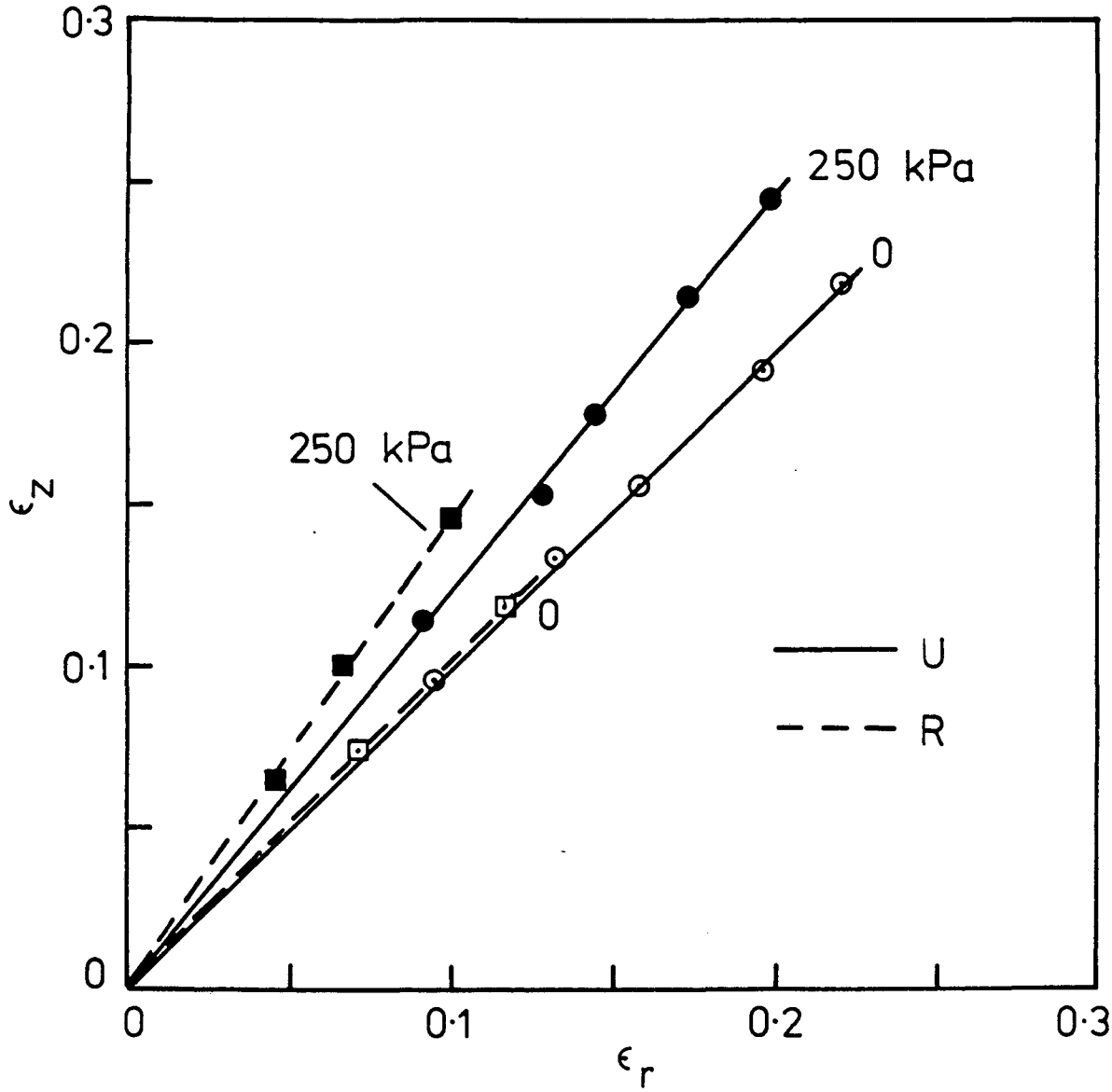

XBL 893-907

Fig. 2

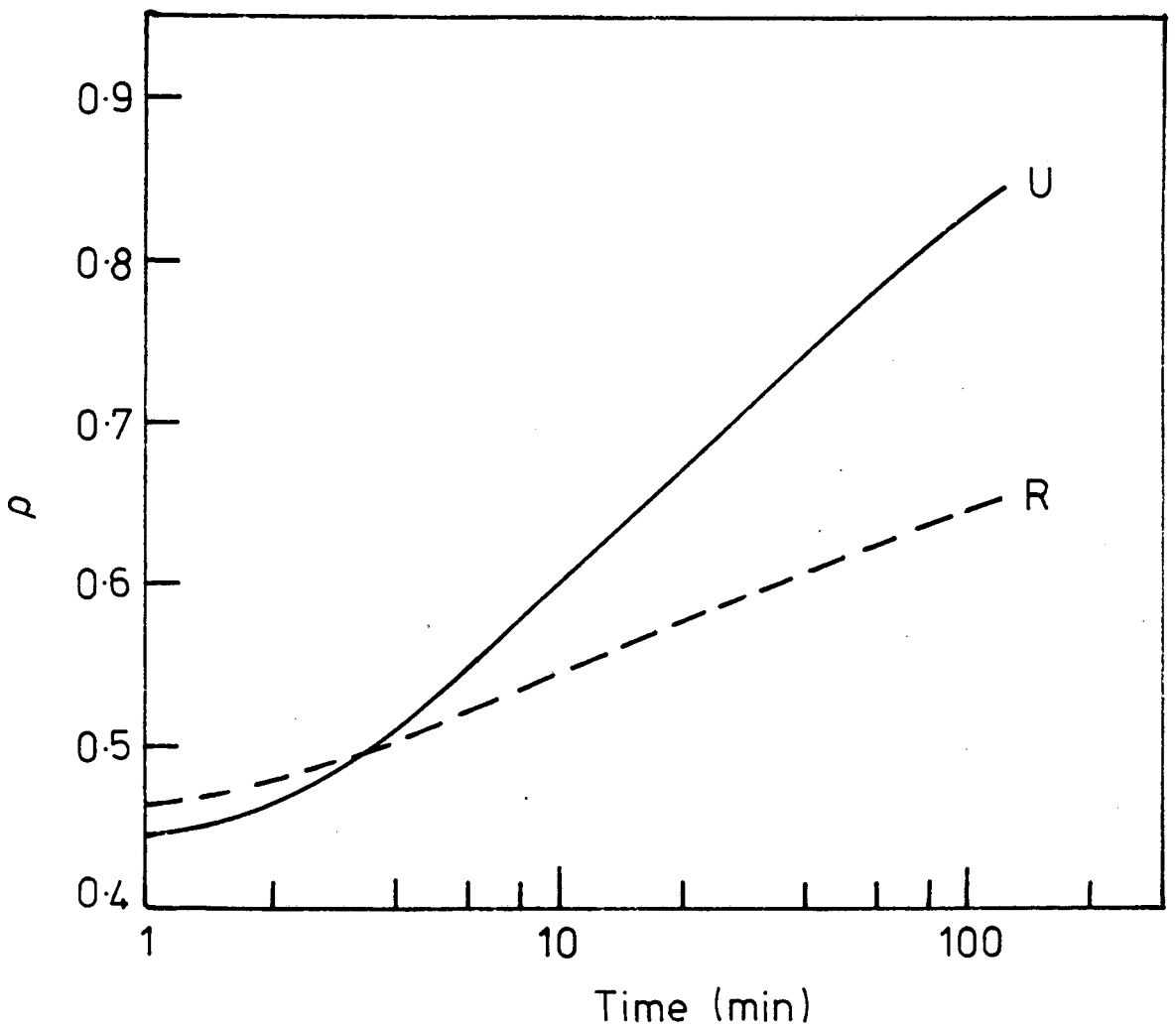

XBL 893-908

Fig. 3

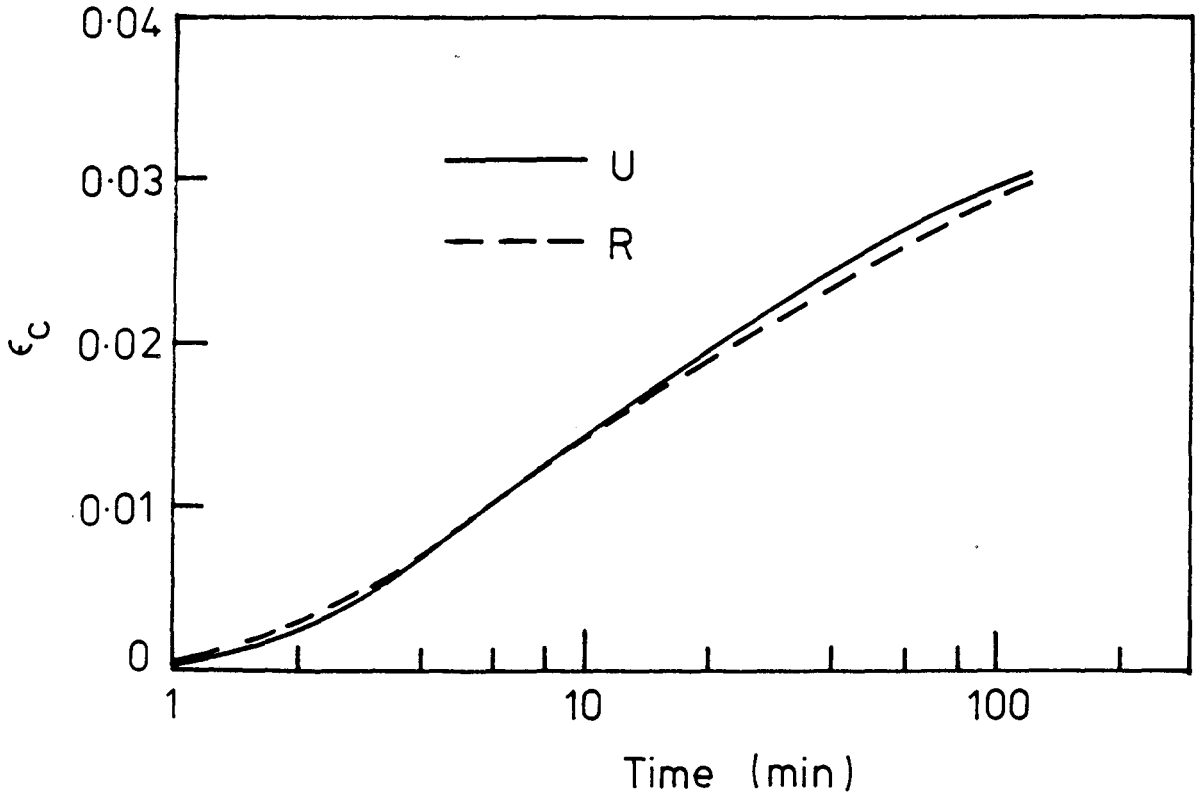

XBL 893-909

Fig. 4

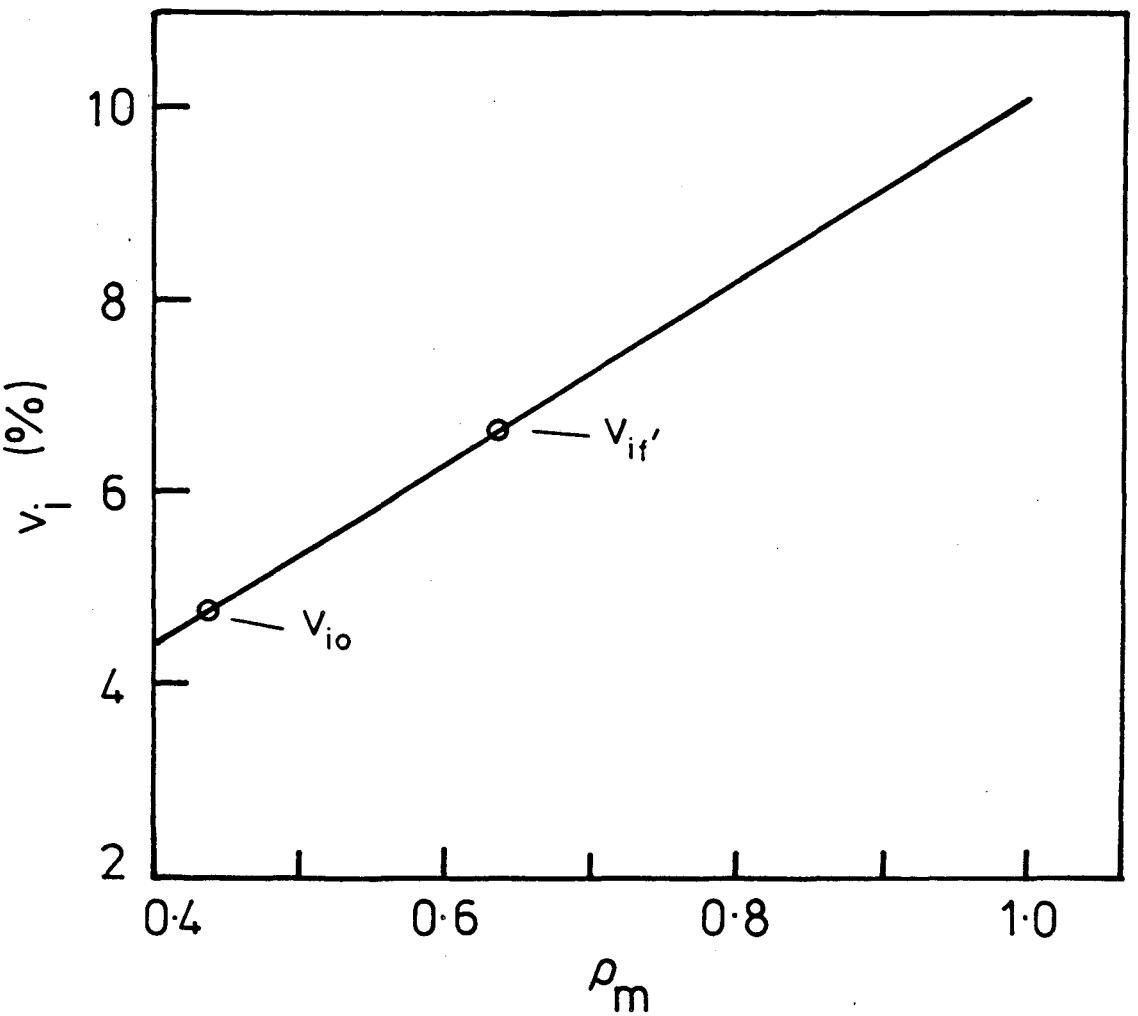

XBL 893-910

Fig. 5

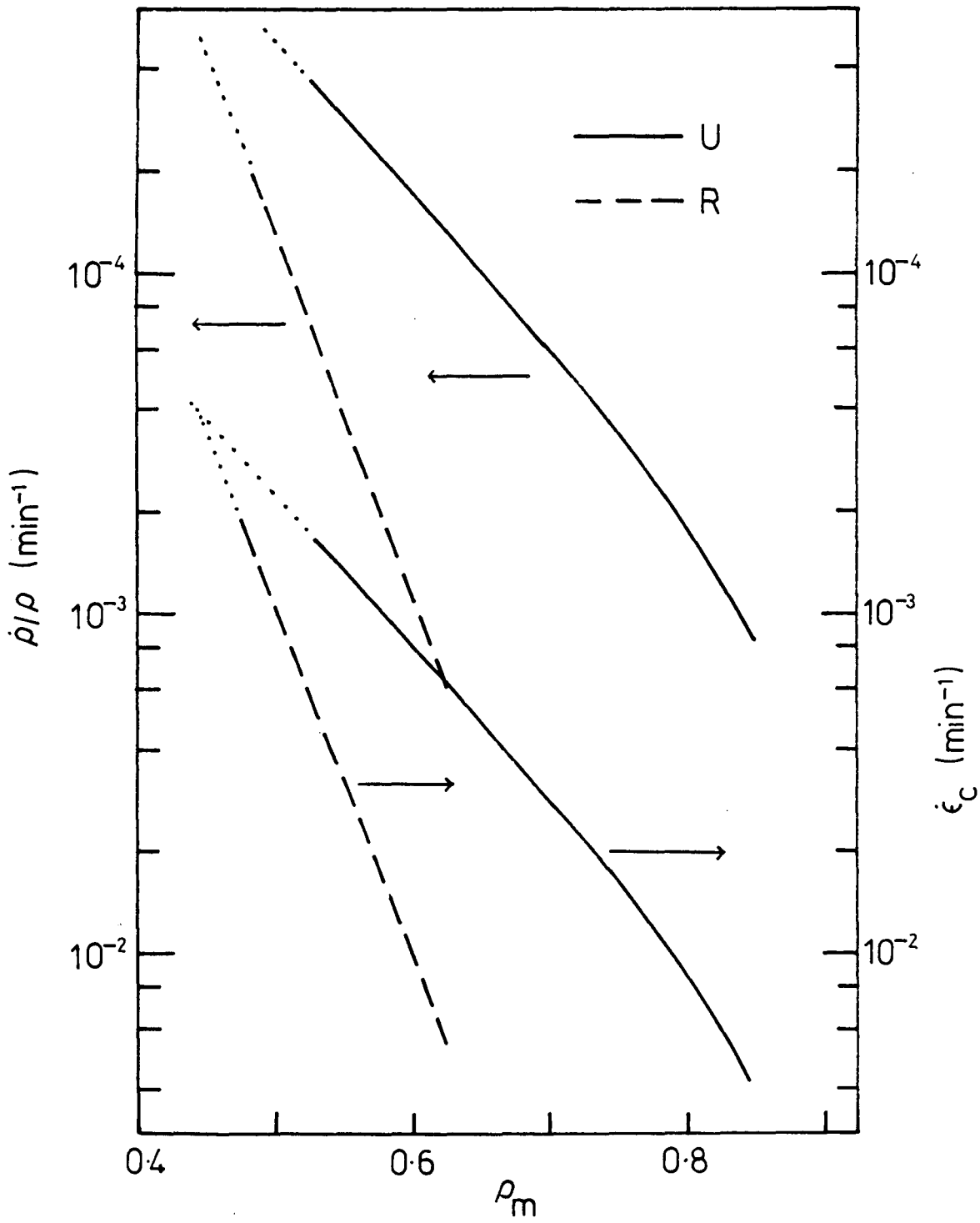

XBL 893-911

Fig. 6

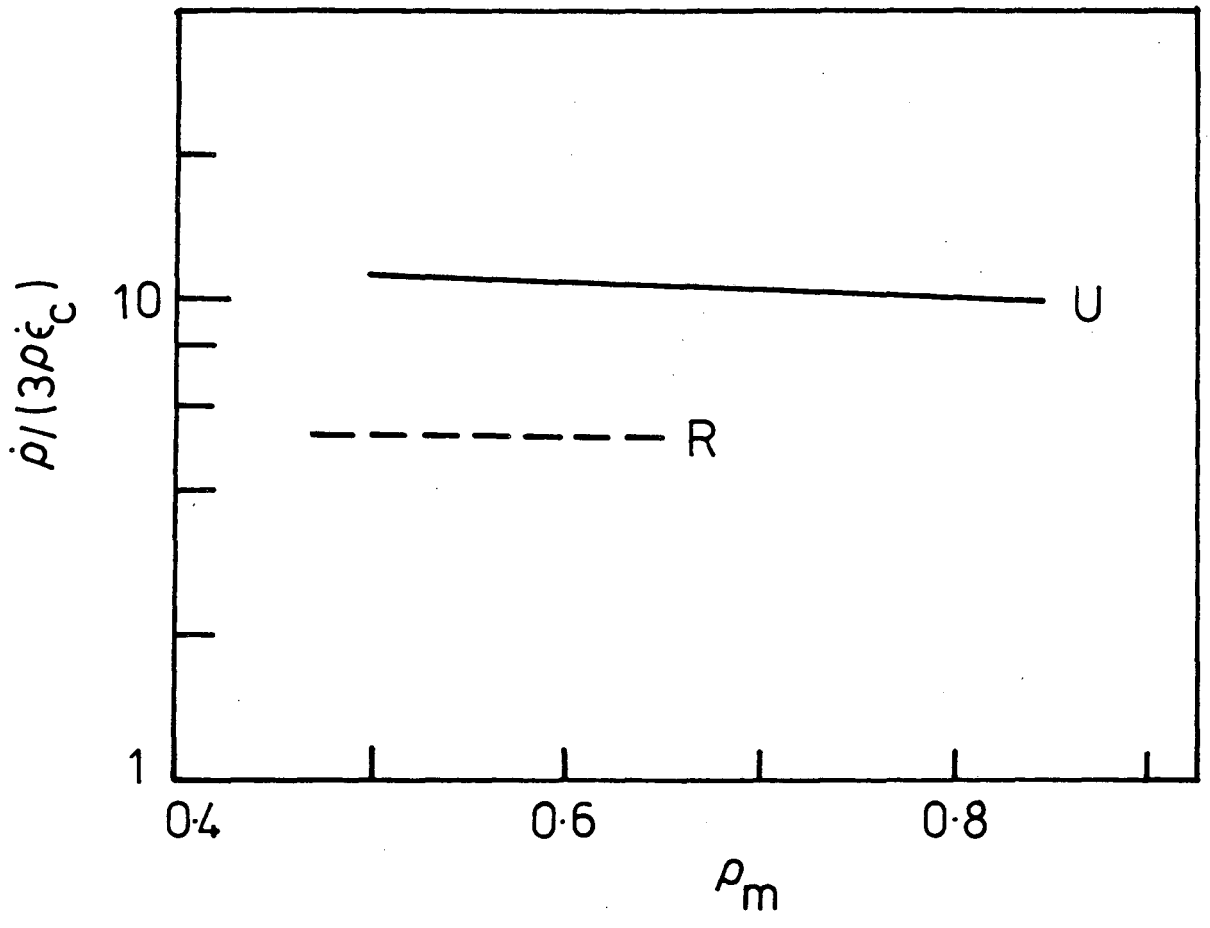

XBL 893-912

Fig. 7

LAWRENCE BERKELEY LABORATORY
TECHNICAL INFORMATION DEPARTMENT
1 CYCLOTRON ROAD
BERKELEY, CALIFORNIA 94720